RESEARCH PAPER

Channels 7:2, 97–108; March/April 2013; © 2013 Landes Bioscience

# Shab $K^+$ channel slow inactivation

## A test for U-type inactivation and a hypothesis regarding $K^+$-facilitated inactivation mechanisms

Elisa Carrillo,† Imilla I. Arias-Olguín,† León D. Islas and Froylan Gómez-Lagunas*

Departamento de Fisiología; Facultad de Medicina; Universidad Nacional Autónoma de México (UNAM); México City, D.F. México

†These authors contributed equally to this work.

**Keywords:** Shab, potassium channels, slow inactivation, U-type inactivation, C-type inactivation, *Drosophila*

Herein, we report the first characterization of Shab slow inactivation. Open Shab channels inactivate within seconds, with two voltage-independent time constants. Additionally, Shab presents significant closed-state inactivation. We found that with short depolarizing pulses, shorter than the slowest inactivation time constant, the resulting inactivation curve has a marked U-shape, but as pulse duration increases approaching steady-state conditions, the U-shape vanishes and the resulting inactivation curves converge to the classical Boltzmann $h_\infty$ curve. Regarding the mechanism of inactivation, we found that external $K^+$ and TEA facilitate both open- and closed-state inactivation, while the cavity blocker quinidine hinders inactivation. These results together with our previous observations regarding the $K^+$-dependent stability of the $K^+$ conductance, suggest the novel hypothesis that inactivation of Shab channels, and possibly that of other Kv channels whose inactivation is facilitated by $K^+$, does not involve a significant narrowing of the extracellular entry of the pore. Instead, we hypothesize that there is only a rearrangement of a more internal segment of the pore that affects the central cavity and halts $K^+$ conduction.

### Introduction

In response to a sustained depolarization, most voltage-gated ion channels open and thereafter inactivate. Inactivation is customarily divided into fast or slow depending on its mechanism and the time scale in which it develops. Slow inactivation is a complex process that develops from the open state over a time course of hundreds of milliseconds to several seconds. The mechanism of slow inactivation is not fully understood and may vary in different channel types.

At first sight slow inactivation may seem too slow to be physiologically relevant; however, it can also develop from closed states and have a slow recovery, producing cumulative inactivation in the time scale of cell signaling.[1,2] Additionally, when both fast and slow inactivation mechanisms are present they can be coupled.[3,4]

Among Kv channels, the most extensively studied form of slow inactivation is that present in the *Drosophila* Shaker B channel, termed C-type inactivation by Aldrich's laboratory because of its dependency on residues present toward the C-terminus domain of the protein.[3] C-inactivation has also been documented in other Kv channels such as HERG and channels of the mammalian Kv1 family.[5]

Shaker C-inactivation develops from the open state with a time constant of ~1–2 sec, in physiological $[K^+]$.[3,6] A hallmark of C-inactivation is its inhibition by external $K^+$ ($K_o^+$) and tetraethylammonium ($TEA_o$) ions.[4,6-9] These, along with other observations,[10] lead to the paradigm that during C-inactivation there is a localized closing or narrowing on the extracellular vestibule of the pore, around Shaker residue 449,[6-13] a key determinant of the $TEA_o$ binding site on the channels.[9,14,15] Accordingly, this region of the external vestibule of the pore has come to be referred to as the C-type inactivation gate. $K^+_o$ and $TEA_o$ are thought to inhibit C-type inactivation by sterically hindering the closing of this gate.[5,10,16]

Other observations indicate that along with the localized constriction on the external vestibule of the pore, C-inactivation may recruit a larger conformational change that affects the selectivity filter (e.g., refs. 17–21) as well as locations along the S6 segment (e.g., refs. 3, 22–25), in particular the central cavity of the pore. Regarding the latter, and of particular interest to this study, is the recent demonstration that internal TEA ($TEA_i$) inhibits the slow inactivation of Kv2.1 and Shaker channels.[26,27]

Another protein domain that has been considered to be engaged in slow inactivation gating is the voltage sensor, since inactivation during a long depolarization, is accompanied with a shift of the gating-charge (Q) vs. voltage (V) curve toward hyperpolarized potentials.[28,29] The term P/C inactivation is used

*Correspondence to: Froylan Gómez-Lagunas; Email: froylangl@yahoo.com
Submitted: 09/19/12; Revised: 01/09/13; Accepted: 01/10/13
http://dx.doi.org/10.4161/chan.23569

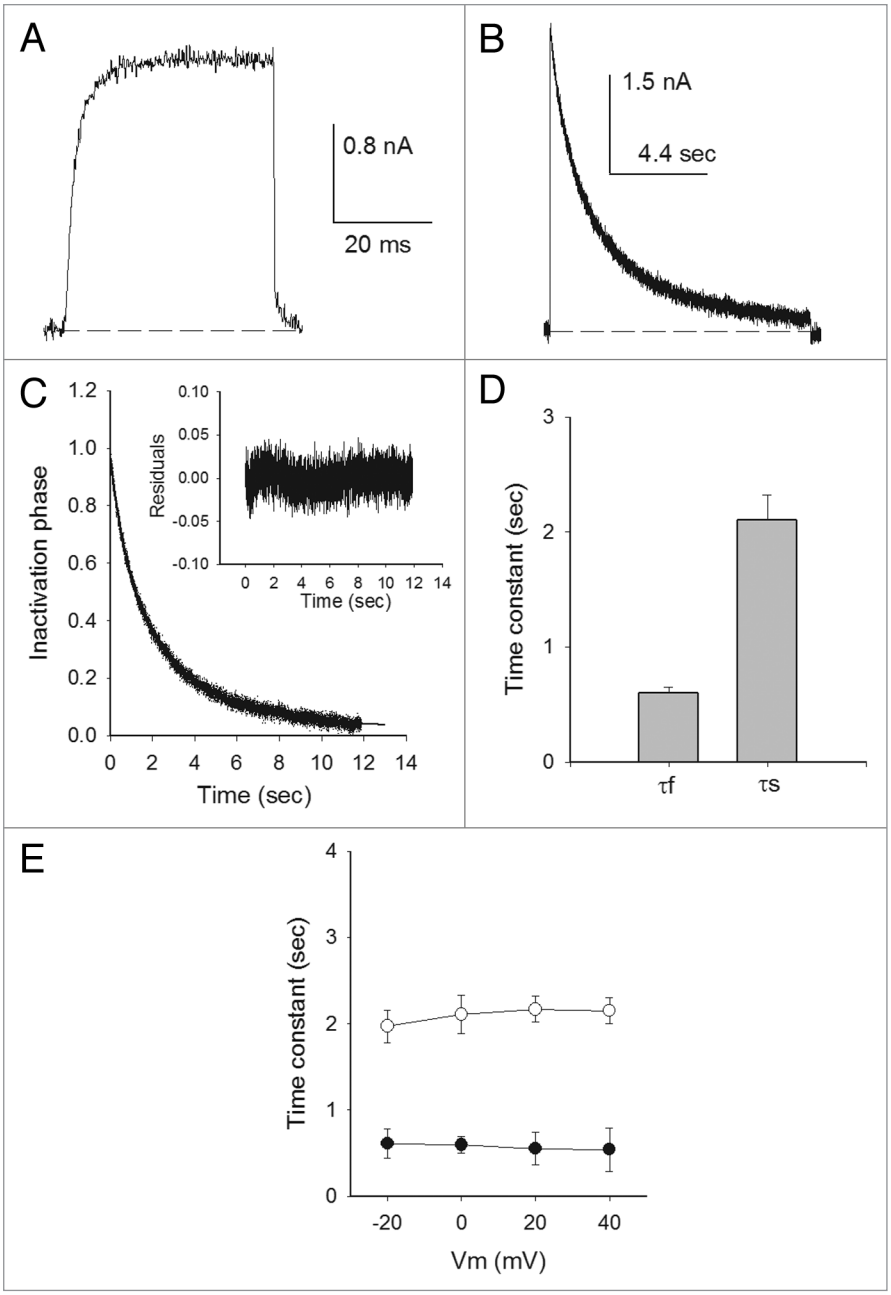


**Figure 1.** Open state inactivation. (**A**) Ik evoked by a 30 ms pulse to 0 mV ($Na_o/K_i$). (**B**) $I_K$ evoked by a 12 sec pulse as in (**A**). (**C**) Normalized inactivation phase of $I_K$ in (**B**), fitted with the equation (solid line): $Ik(t)/Io = Af_{Na}*\exp(-t/\tau_{f,OI,Na}) + As_{Na}*\exp(-t/\tau_{s,OI,Na}) + C_{Na}$; where: Io is peak $I_K$; $Af_{Na} = 0.39$, $\tau_{f,OI,Na} = 0.83$ sec; $As_{Na} = 0.55$, $\tau_{s,OI,Na} = 3.2$ sec; and $C_{Na} = 0.03$ (see text). The inset shows the residuals of the fit. (**D**) Inactivation time constants at 0 mV, obtained as in (**B**). (**E**) Fast (closed symbols) and slow (open symbols) time constants vs. Vm n = 8.

to distinguish between the change(s) in the pore and the accompanying change in the voltage sensor.[5,30] Nonetheless, recent observations have suggested that inactivation and the shift of the Q-V curve may not be causally related, but that the latter might be an intrinsic property of voltage sensors.[31]

Some Kv channels present a slow inactivation whose properties differ from those distinctive of the canonical C-inactivation of Shaker. An example is Kv2.1, a mammalian ortholog of Shab, which presents an inactivation that preferentially arises from partially activated closed states, follows a U-shaped inactivation curve, and therefore has been termed U-type inactivation.[32,33] In addition to Kv2.1, other Kvs including Kv1.3 and truncated Kv1.5 channels,[5,34] have also been reported to present U-type inactivation.

In contrast to its inhibitory effect on C-inactivation, $K_o^+$ slightly accelerates the open-state inactivation (OI) of both Kv2.1 and Kv1.3 channels, although it slows down, and in a more prominent manner, the dominant closed-state inactivation (CI) of Kv2.1 channels.[26,32,34] On the other hand, $TEA_o$ has no effect either on OI or CI of Kv2.1.[26] It is noteworthy that, to our knowledge, no mechanism has been proposed to explain the facilitation of inactivation exerted by $K_o^+$ in these channels.[5]

In contrast to the extensive studies performed to characterize the *Drosophila* Shaker channel inactivation, the inactivation of the related Shab channels[35,36] has escaped attention. This has occurred in spite of a wealth of evidence indicating significant roles of Shab channels in membrane excitability, for example in action potential repolarization, and repeated spiking in a variety of *Drosophila* muscle and neural cells, as well as in cardiac beat frequency.[37-43] Clearly, in order to best understand the role of Shab in cell physiology, knowledge of its inactivation gating is required. Additionally, this will undoubtedly increase our understanding of inactivation mechanisms and pore dynamics of Kv channels.

Herein, we report the first characterization of the slow inactivation gating of delayed rectifier Shab channels and a critical test for U-type inactivation. Additionally, a novel hypothesis regarding the mechanism of $K^+$-facilitated inactivation process is stated.

## Results

Once open, Shab $K^+$ channels undergo a slow inactivation process that develops over seconds.[36] This is illustrated in **Figure 1** which presents potassium currents ($I_K$) evoked either by a short, 30-ms, depolarization to 0 mV (**Fig. 1A**), or by a long, 12 sec, pulse to the same voltage (**Fig. 1B**), in cells bathed in $Na_o/K_i$ control solutions (see *Materials and Methods*). In contrast to $I_k$ evoked with the short pulse, which does not decay, when the membrane is maintained depolarized for 12 sec, $I_K$ gradually decays as channels slowly inactivate from the open state.

The time course of Shab open-sate inactivation (OI) is best fitted with the sum of two exponentials than with a simpler single exponential model ($p < 0.001$). This is illustrated in **Figure 1C** which shows the fit of the normalized inactivation phase of $I_k$ in **Figure 1B** (solid line), with a fast time constant $\tau_{f,OI,Na}$ = 0.84 sec (average, 0.6 ± 0.1 sec; see **Fig. 1D**), with relative amplitude $Af_{Na}$ = 0.42 (average, 0.3 ± 0.04); and a slow time constant $\tau_{s,OI,Na}$ = 3.3 sec (average, 2.1 ± 0.2 sec), with relative amplitude $As_{Na}$ = 0.6 (average, 0.68 ± 0.03), plus a constant $C_{Na}$ = 0.03 term (average, 0.05 ± 0.01, n = 8). The inset shows the residuals of the fit. As commonly found in several types of inactivation, both fast and slow, **Figure 1E** shows that at fully activating potentials (≥ –20 mV) both time constants are not appreciably voltage-dependent.

Shab $\tau_{s,OI,Na}$ has a value similar to the time constant of the Shaker C-type inactivation in equivalent ionic conditions,[6] and faster than that of its mammalian ortholog Kv2.1 channel.[32] Considering that the latter presents a U-type inactivation, our next goal was to determine if Shab presents its defining characteristic, namely a U-shaped inactivation curve.

**Shab inactivation curve: A test for U-type inactivation.** In order to determine if Shab presents U-type inactivation the Shab inactivation curve was analyzed, applying depolarizing pulses of variable duration, using both a modified three-pulse protocol and a standard two-pulse protocol. In the first one, a control pulse was initially applied ($V_{control}$ = +40 mV/30 ms). Thereafter, a pulse (pre-pulse) of variable amplitude and duration was delivered. Finally, a test pulse was applied ($V_{test} = V_{control}$), and inactivation was evaluated as the ratio of the currents evoked by the last and the first pulse, $I_{K,test}/I_{K,control}$.

The standard protocol lacked the first control pulse, and inactivation was assessed as $I_K(V)/I_{K,max}$, where $I_{K,max}$ is the maximal $I_K$ measured during the second test pulse that was applied immediately after delivering the first pre-pulse of the indicated amplitude and durations. Both protocols yielded identical results (see below) due to the lack of variation of $I_K$ in the first pulse of the three-pulse protocol (not shown, but noticeable in **Fig. 2A** right panel).

**Figure 2A** left panel is a plot of the extent of inactivation (non-inactivated fraction) reached with the delivery of inactivating pulses of increasing duration (0.05, 0.9, 3 and 5 sec, as indicated), applying either the two (closed symbols) or the three-pulse (open symbols) protocols. As expected, very short depolarizations, lasting only 0.05 sec, produce a quite small inactivation at all of the voltages tested. Nonetheless, it is seen that the points of the resulting inactivation curve show a slight hint of a U-shape.

When pulse duration is increased to 0.9 sec the extent of inactivation increases and the points in the curve acquire a marked U-shape,[5,32-34] with a well-defined minimum at –20 mV. The latter is illustrated by the traces in the right panel which depict two superimposed $I_K$ obtained with the three-pulse protocol with pre-pulse of either –20 mV/0.9 s or +20 mV/0.9 s, as indicated. Note that as observed in the curve, $I_{K,test}$ at +40 mV following the +20 mV pre-pulse is notably larger than $I_{K,test}$ following the –20 mV pre-pulse. Finally, and importantly: observe that because of the slow kinetics of inactivation (**Fig. 1**), a 0.9 sec pulse is clearly not sufficiently long to approach steady-state conditions.

When pulse duration is further increased to 3 and 5 sec, and thus steady-state inactivation is progressively approached, two facts are observed: first, the extent of inactivation increases, and second, and more interesting, the marked U-shape of the points observed with the shorter 0.9 sec pulses, becomes less evident (**Fig. 2A**).

The U-shape completely disappears when the pulse duration is significantly increased (**Fig. 2B**, left panel) to 20 sec (~10 times the slowest inactivation time constant, **Fig. 1** and see below), yielding near steady-state conditions, under which the inactivation curve follows the classical $h_\infty$ Boltzmann equation. This is also noted in the inset, which compares the curves obtained with 3 sec (duration ~$\tau_{s,OI,Na}$) and 20 sec pre-pulses (duration > > $\tau_{s,OI,Na}$). The same $h_\infty$ Boltzmann-curve is obtained both with $Na_o$ or 100 mM $K_o$ solutions.[44] The right panel serves to illustrate $I_K$ behavior with 20 sec pre-pulses, by showing two superimposed $I_K$ evoked with the 3-pulse protocol applying either –20 or +20 mV. Notice that the corresponding $I_K$, at the final test pulse of +40 mV, have a size difference that is hardly distinguishable from the noise, as clearly seen with the expanded scale of the inset (indicated by the arrow).

In contrast to U-type curves, which present a sizable positive slope at positive potentials, the Boltzmann equation, which fits Shab inactivation under near steady-state conditions, approaches 0 when $V > > V_{1/2}$. This is illustrated in **Figure 2C**, which plot the chord slope obtained with the average relative currents following pre-pulses of –20 and +20 mV $\{[I_{rel}(+20\ mV)-I_{rel}(-20\ mV)]/40\}$, of the indicated duration, as in **Figure 2A and B**. The magnitude of the slope provides a measurement of departure from a Boltzmann relation, in other words it serves to indicate how marked is the U-shape character of the corresponding curve. Note that as pre-pulse duration increases, approaching near steady-state conditions, the slope falls steeply toward 0, as contained in the Boltzmann equation. The open circle departs from the general tendency of the remaining points (closed circles). This point corresponds to 0.05 sec pre-pulses, too short to produce a significant inactivation (**Fig. 2A**).

It is clear that the U-shape of the inactivation curves as in **Figure 2A** are due to kinetic processes, which are the result of being far from steady-state conditions (see ref. 45 and *Discussion*). After rejecting U-inactivation, as the type of inactivation present in Shab channels, our next goal was to determine whether Shab presents the characteristic features of C-type inactivation.

**Shab inactivation is not C-type: Effects of $TEA_o$ and $K_o^+$ on OI.** In order to determine if inactivation follows a C-type mechanism, the effects of $TEA_o$ and $K_o^+$ on open state inactivation (OI) were determined by applying 7 sec pulses, that open and inactivate the channels, to cells bathed in either TEA or $K^+$-containing external solutions. **Figure 3A** presents the outcome of adding TEA to the external solution. The traces in the left panel compare representative $I_K$ recorded either in the reference $Na_o$ solution (larger trace, labeled Na) or with 15 mM $TEA_o$ (smaller trace, labeled TEA), a concentration that inhibits ~50% of channels.

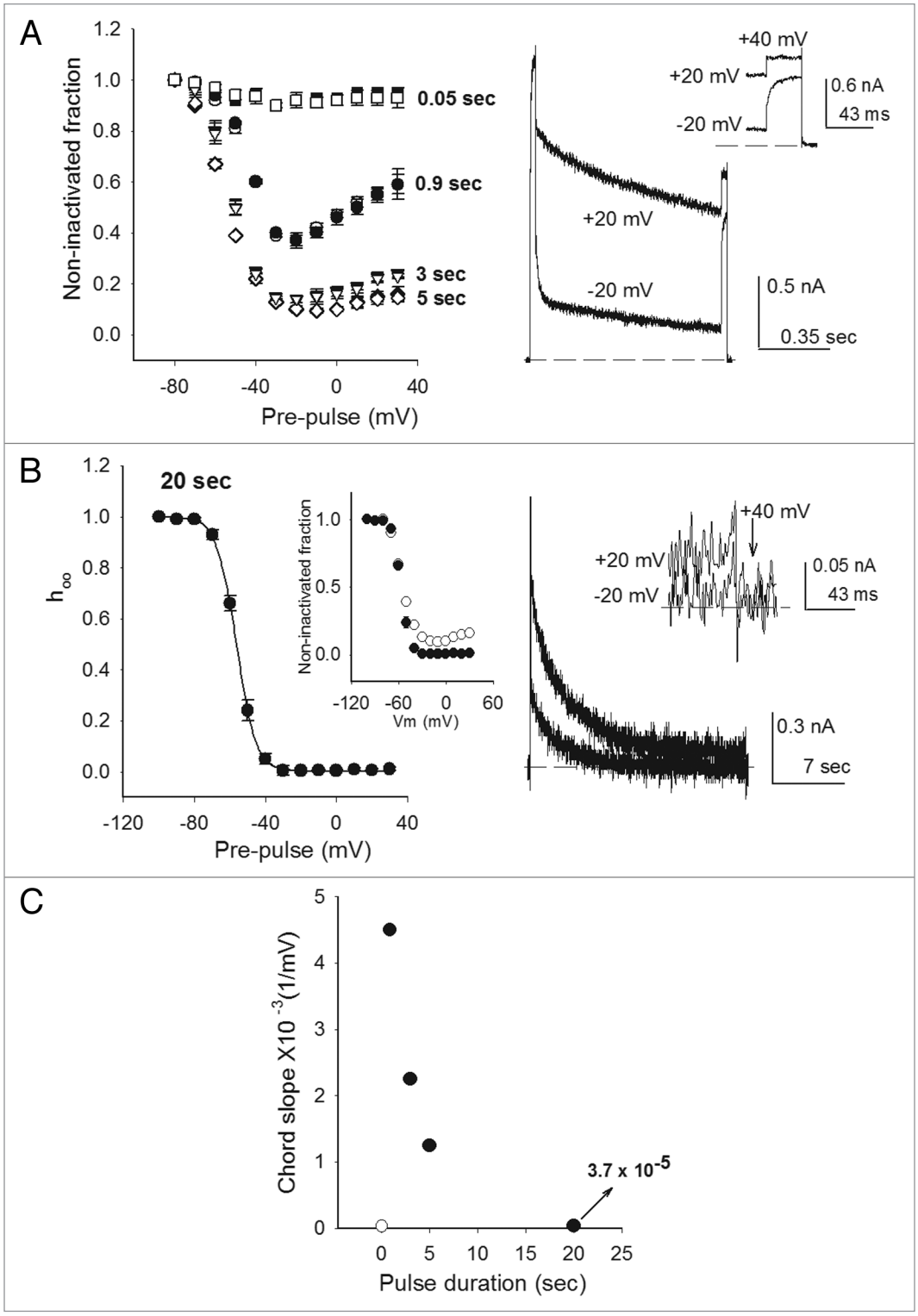


**Figure 2.** Inactivation curve under far and near steady-state conditions. (**A**) Left panel, inactivation promoted with short depolarizing pulses, as indicated. Inactivation was assessed with either a three (closed symbols) or a two pulse protocol (open symbols) (see text). Right panel, superimposed $I_K$, obtained with the three-pulse protocol, applying a –20 or a +20 mV pre-pulse of 0.9 sec duration, as indicated. The inset shows $I_K$ evoked by the final test pulse in an expanded scale. (**B**) Left panel, $h_\infty$ inactivation curves (data from ref. 44). The curve was obtained applying 20-sec pre-pulses of the indicated amplitude in $Na_o$ solutions. The line is the fit of the points with the Boltzmann equation $h_\infty = 1/(1+\exp[(zF/RT)(Vm-V_{1/2})])$, with parameters $V_{1/2}$ = -56.3 mV, z = 4.6. Inset: inactivation after either 3- (open circles) or 20- sec pulses (closed circles). Right panel, superimposed $I_K$ recorded as in (**A**) right panel, but applying either –20 or +20 mV pulses of 20 sec duration, as indicated. The inset shows $I_K$ evoked by the final, +40 mV, test pulse (arrow) in an expanded scale. (**C**) Inactivation curve chord slope, between –20 and +20 mV, as a function of pre-pulse duration. Points are mean ± SEM of at least four experiments.

In order to facilitate its comparison, $I_K$ with $TEA_o$ was scaled to the peak $I_K$ in 0 $TEA_o$ (middle trace). As observed in $Na_o$ solutions (**Fig. 1**), OI in the presence of $TEA_o$ also follows a two exponential time course (right panel), but it is seen that in this condition, Shab OI becomes noticeably faster. This is quantified in the histogram on the right panel, which compares inactivation time constants in $Na_o$, with those obtained with 15 mM $TEA_o$. Notice that $TEA_o$ significantly decreases (~44%) both the fast (p = 0.02, n = 4) and the slow (p = 0.023, n = 4) OI time constants, without significantly changing their relative amplitudes.

$TEA_o$ facilitation of Shab inactivation is in clear contrast to its opposite, inhibitory, effect on C-inactivation,[6-9] and to its lack of effect on the inactivation of the Kv2.1 channel.[26]

Next we investigated the role of $K_o^+$ on Shab OI. **Figure 3B** left panel compares $I_K$ evoked by a +20 mV/7 sec pulse with the cell bathed in 100 $K_o^+$ (smaller $I_K$, labeled K) against $I_K$ recorded in the same cell bathed in 0 $K_o$ solution (trace labeled Na). $I_K$ in 100 $K_o$ is much smaller than in 0 $K_o$, because with 100 mM $K_o^+$ the pulse voltage is near the $K^+$ equilibrium potential. Therefore, to compare their kinetics the trace in 100 $K_o^+$ was scaled to peak $I_K$ in 0 $K_o^+$ (middle trace). Note that, in contrast to its known inhibitory effect on C-type inactivation, $K_o^+$ clearly speeds Shab OI. Quantitation is reported in the right panel which shows that $K_o^+$ significantly decreases (~30%) both the fast (p = 0.027) and the slow (p = 0.019) time constants. This speeding-up occurred without a significant change in the relative amplitudes of their corresponding OI phases (see figure legend), as seen with $TEA_o$.

$TEA_o$ blocks $I_k$ in 100 $K_o^+$ as effectively as in 0 $K_o^+$ (not shown), therefore we wondered whether the individual effects of 15 mM $TEA_o$ and 100 mM $K_o^+$ could be additive. The superimposed traces in **Figure 3C** illustrate that, unexpectedly, they are not (the same result was observed in at least two other cells, see *Discussion*). The above observations are summarized in **Figure 3D** which, for clarity, presents the plot of the least squares curves that fit OI, in the indicated conditions.

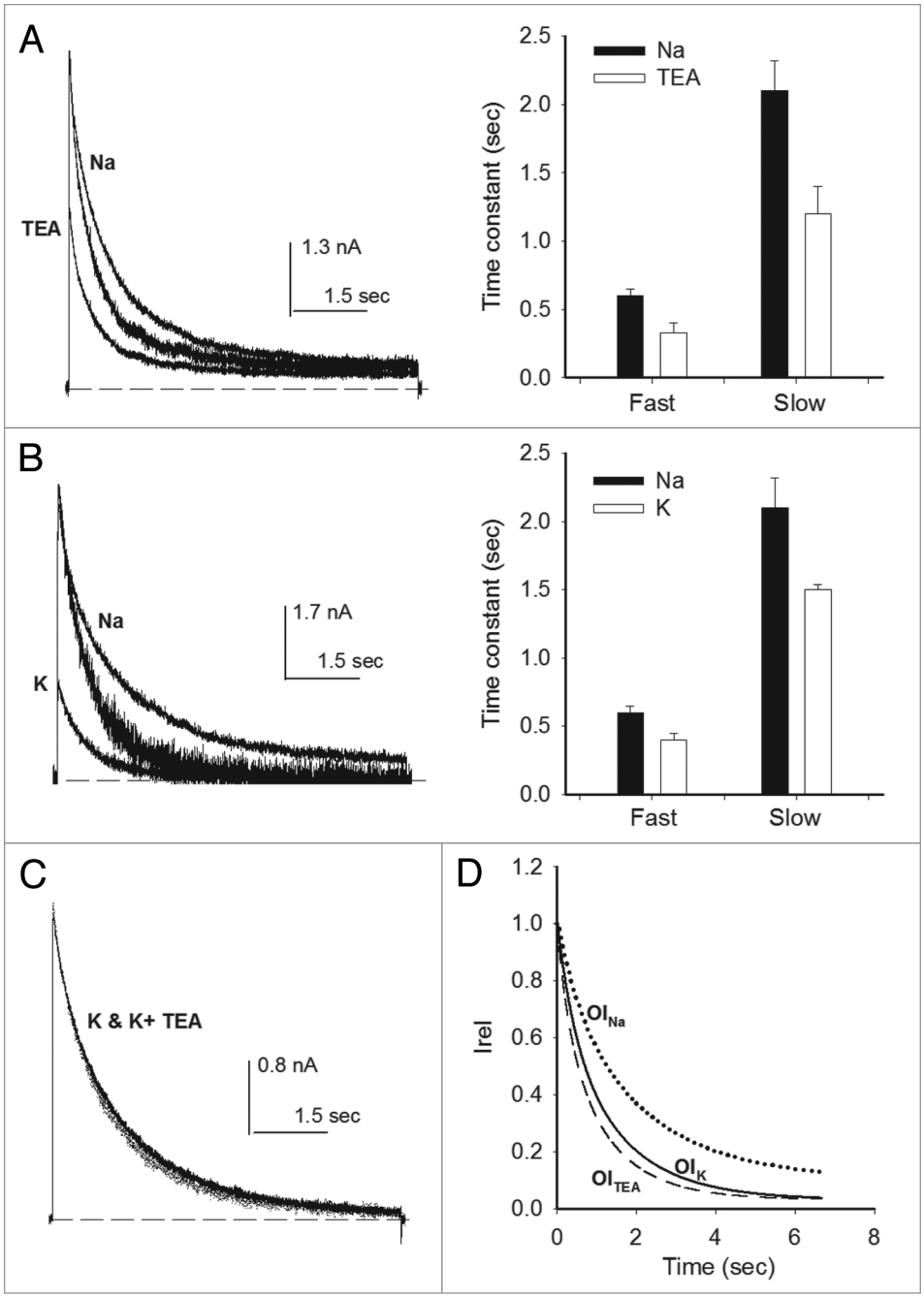


**Figure 3.** Effects of $TEA_o$ and $K_o^+$ on OI. (**A**) Left panel, $I_K$ evoked by 0 mV/7 sec pulse applied either in the absence ($Na_o$) or in the presence of 15 mM $TEA_o$, as indicated. Middle trace: $I_K$ with TEA scaled to control peak $I_K$. OI follows the time course (**Fig. 1**): $Ik(t)/Io = Af*\exp(-t/\tau_{f,OI}) + As*\exp(-t/\tau_{s,OI}) + C$; Io is peak $I_K$; $\tau_{f,OI,TEA} = 0.33 \pm 0.07$, $\tau_{s,OI,TEA} = 1.2 \pm 0.22$, $Af_{TEA} = 0.28 \pm 0.07$, $As_{TEA} = 0.65 \pm 0.07$, $C_{TEA} = 0.06 \pm 0.02$. Right panel, inactivation time constants measured either in $Na_o$ or in 15 mM $TEA_o$. $TEA_o$ significantly decreases both constants ($p < 0.05$). (**B**) Left panel, $I_K$ evoked by a +20 mV/7 sec pulse applied in either $Na_o$ or 100 $K_o$ solutions, as indicated. Middle trace: $I_K$ in 100 $K_o$ scaled to control peak $I_K$. Right panel, inactivation time constants, as indicated. (**C**) Superposed $I_K$ recorded in either 100 mM $K^+_o$ or in 100 $K^+_o$ plus 15 mM $TEA_o$. (**D**) OI time course. The lines are the least squares fit of OI of traces as in (**A and B**): 15TEA (dotted line, parameters as above, n = 6); 100 Ko (dashed line, n = 6): $\tau_{f,OI,K} = 0.4 \pm 0.05$ sec, $\tau_{s,OI,K} = 1.5 \pm 0.04$ sec, $Af_K = 0.34 \pm 0.13$, $As_K = 0.64 \pm 0.12$, $C_K = 0.02 \pm 0.008$; $Na_o$ (solid line): $\tau_{f,OI,Na} = 0.6 \pm 0.05$ sec, $\tau_{s,OI,Na} = 2.1 \pm 0.22$, $Af_{Na} = 0.3 \pm 0.02$, $As_{NA} = 0.68 \pm 0.03$, $C_{Na} = 0.05 \pm 0.01$.

The former observations show that Shab inactivation presents properties opposite to those characteristic of the C-type inactivation mechanism. Also, it is important to point out that: the facilitation exerted by $TEA_o$ and $K_o^+$ does not by itself suggest an inactivation mechanism involving a closing or significant narrowing of the extracellular entry of the pore.

Our next goal was to determine if Shab presented closed state inactivation (CI), and whether the pore had to open for $K^+$ and TEA to be able to affect inactivation.

**Inactivation from closed states.** We determined the extent and kinetics of closed-state inactivation by assessing the cumulative inactivation produced by short 20-ms repeated pulses of either 0 or +20 mV, which activate the channels without allowing the development of significant OI, applied at a rate that precluded significant recovery from inactivation between consecutive pulses ($1.3 \times 10^{-4}$ Hz).

**Figure 4A** illustrates $I_K$ obtained with the above protocol, in the reference $Na_o/K_i$ solutions. For clarity only the first $I_K$ recorded are shown. Note that, although none of the currents presents a noticeable OI, $I_K$ decreased with each consecutive pulse, therefore indicating the presence of closed state inactivation ($CI_{Na}$). This is best seen in **Figure 4B** which presents the average relative $I_K$ as a function of the number of pulses.

In order to determine CI kinetics, the points in **Figure 4B** were plotted as the average relative $I_K$ vs. time (**Fig. 4C**). $CI_{Na}$ follows a single exponential time course (solid line), with time constant $\tau_{CI,Na} = 0.61$ sec, plus a constant term $C_{Na} = 0.39$, which accounts for the fraction of channels that do not manage to inactivate during their transit along closed states, at this voltage. Note that, interestingly, $\tau_{CI,Na}$ at −80 mV is basically identical to the fast $OI_{Na}$ time constant (**Fig. 1**), which accounts for ~30% of $OI_{Na}$. This is easily observed in **Figure 4C** which for comparison also presents the curve that describes $OI_{Na}$ time course (dashed line).

The former observations show that, in contrast to Shaker which mainly inactivates from the open state, Shab inactivates from both open and closed states, but in contrast to its ortholog Kv2.1, Shab channels do not preferentially inactivate from closed states.

Next we investigated whether channels have to open for its inactivation to be modulated by $K_o^+$ and $TEA_o$. **Figure 4D** shows the plot of the average relative $I_K$ vs. time, obtained with the above protocol in cells bathed in 100 $K_o^+$ (closed circles). $I_K$ falls along an exponential time course (solid line), as channels inactivate from closed states, with time constant $\tau_{CI,K} = 0.4$ sec, plus a constant term $C_k = 0.2$. Importantly, $CI_K$ is significantly faster and therefore more complete ($p < 0.01$), than $CI_{Na}$. The latter is visually appreciated in the figure which, for a reference, also presents the time course of $CI_{Na}$ (dotted line). Finally, notice that $\tau_{CI,K}$ at −80 mV is basically equal to $\tau_{f,OI,K}$ (dashed line), as previously also observed in $Na_o$ (**Fig. 4C**).

The role of $TEA_o$ on closed state inactivation is presented in **Figure 4E**, which shows CI in cells bathed in 15 mM $TEA_o$ (closed circles). $CI_{TEA}$ follows an exponential time course (solid line through the points) with time constant $\tau_{CI,TEA} = 0.5$ sec, plus a constant term $C_{TEA} = 0.19$. Notice that $CI_{TEA}$ is faster, and hence more complete, than CI in the absence of $TEA_o$ ($CI_{Na}$, dotted line, $p < 0.01$). Also, notice that, as previously found with both $Na_o$ and 100 $K_o$ solutions, $\tau_{CI,TEA}$ is basically identical to $\tau_{f,OI,TEA}$ (dashed line).

**Figure 4F** compares CI in the ionic solutions tested. It is easily appreciated that $CI_{TEA}$ and $CI_K$ are indistinguishable (**Fig. 4F**), and faster and more complete than $CI_{Na}$. These data shows that, at the tested concentrations, $K_o^+$ and $TEA_o$ exert similar effects on both open (**Fig. 3**) and closed state inactivation.

The above observations indicate that $TEA_o$ and $K_o^+$ facilitate Shab inactivation, regardless of the state of the activation gate. This suggest the hypothesis that Shab reaches the same inactivated conformation from either open or closed states, and further indicates that Shab inactivation does not obey a C-type inactivation mechanism.

Interestingly, and related to the latter, recent observations point to the involvement of the central cavity in the slow inactivation gating of several Kv channels, exhibiting both C- and non-C-type inactivation mechanisms. Therefore, we decided to test the effect of adding an intracellular pore blocker that binds to the central cavity on Shab inactivation.

**Inactivation inhibition by the intracellular pore blocker quinidine.** It has been reported that inactivation properties may change upon establishing the inside-out configuration of the patch-clamp technique.[27,46] Therefore, we decided to use quinidine (Qd), as this molecule added to the extracellular solution rapidly equilibrates across the membrane blocking the Shab open pore from the intracellular side of the membrane,[47] allowing tests of Qd effect on inactivation in the whole-cell recording configuration.

In order to evaluate the effect of Qd on Shab inactivation, a 0 mV/7 sec pulse was applied to channels bathed in a control 5 $K_o^+$ solution.[47] Thereafter, Qd was added at either 0.03 or 0.1 mM concentrations in the 5 $K_o^+$ solution, and once it equilibrated across the membrane (not shown), its effect on inactivation was tested.

**Figure 5A** shows two superimposed $I_K$ recorded before (larger $I_K$) and after the addition of 0.1 mM Qd (smaller $I_K$). Qd blocked Shab, markedly reducing $I_K$ amplitude and, more interesting for the present discussion, slowing inactivation when compared with control $I_K$. This is best appreciated in the right panel which presents $I_K$ with Qd normalized to control peak $I_K$. In these superimposed traces, Qd inhibition of inactivation is easily appreciated by comparing $I_K$ size at pulse-end in control vs. in Qd-blocked channels.

The above observation is quantitatively presented in **Figure 5B**, which illustrates the extent of inactivation reached at the end of the inactivating pulse, as in **Fig. 5A** (see figure legend). Note that in the absence of Qd the extent of inactivation (92.6 ± 1.4%, n = 5) is significantly larger than that observed in channels bathed in either 0.03 mM (81.6 ± 4%, n = 5; p = 0.0318), or 0.1 mM Qd solutions (66.8 ± 5%, n = 5; p = 0.0011). Although further work is needed to determine the mechanism by which Qd hinders inactivation, this observation points to the participation of the central cavity of the pore in the slow inactivation gating of Shab channels.

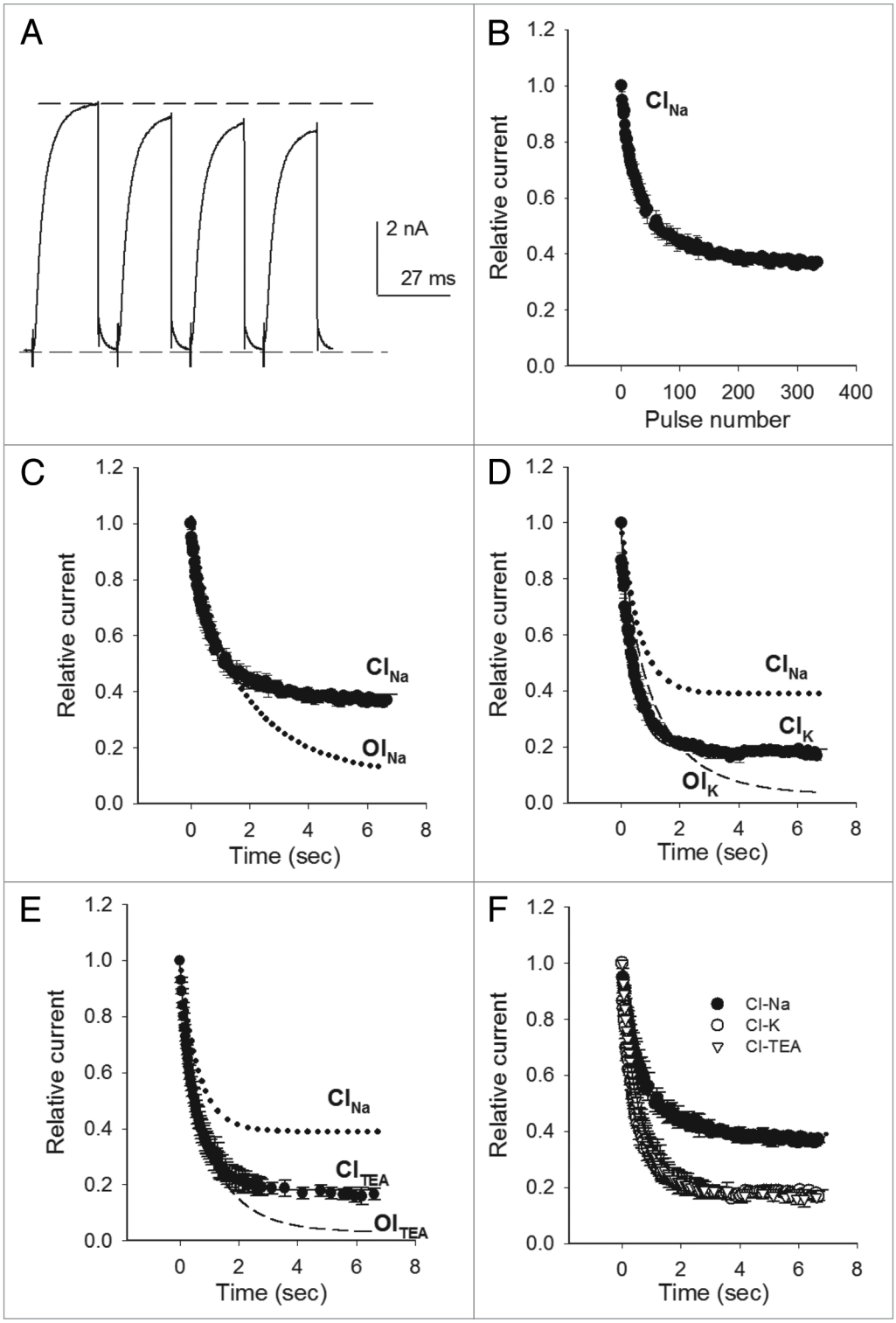


**Figure 4.** Closed state inactivation. (**A**) $I_K$ evoked by four consecutive 0 mV/20 ms pulses, applied at 1.3 x $10^{-4}$ Hz ($Na_o/K_i$). (**B**) Average relative $I_K$ as a function of the number of applied pulses, as in (**A**). (**C**) Points in (**B**) plotted as Relative $I_K$ vs. time ($CI_{Na}$, closed circles). The solid line is the fit of the points with the equation: I/Io = Aexp(-t/τ)+ C, where I is $I_K$ at time t; Io is $I_K$ at t = 0; $\tau_{CI,Na}$ = 0.61 sec, $A_{Na}$ = 0.61, $C_{Na}$ = 0.39. The dotted line is the curve that fits $OI_{Na}$ time course. (**D**) CI time course with 100 $K_o^+$ (closed circles, $CI_K$). The solid line is the least squares fit of the points with $\tau_{CI,K}$ = 0.4 sec, $A_K$ = 0.8 and $C_K$ = 0.19. Dashed line: $OI_K$ time course; dotted line: $CI_{Na}$ time course. (**E**) $CI_{TEA}$: Average relative $I_K$ vs. time, assessed with 15 mM $TEA_o$ (closed circles). The solid line is the fit of the points with $\tau_{CI,TEA}$ = 0.5 sec, $C_{TEA}$ = 0.18 and $A_{TEA}$ = 0.82. Dashed line: $OI_{TEA}$ time course; dotted line: $CI_{Na}$ time course. (**F**) CI time course in the indicated conditions. HP = –80 mV. The points are the mean ± SEM of at least four experiments on each condition.

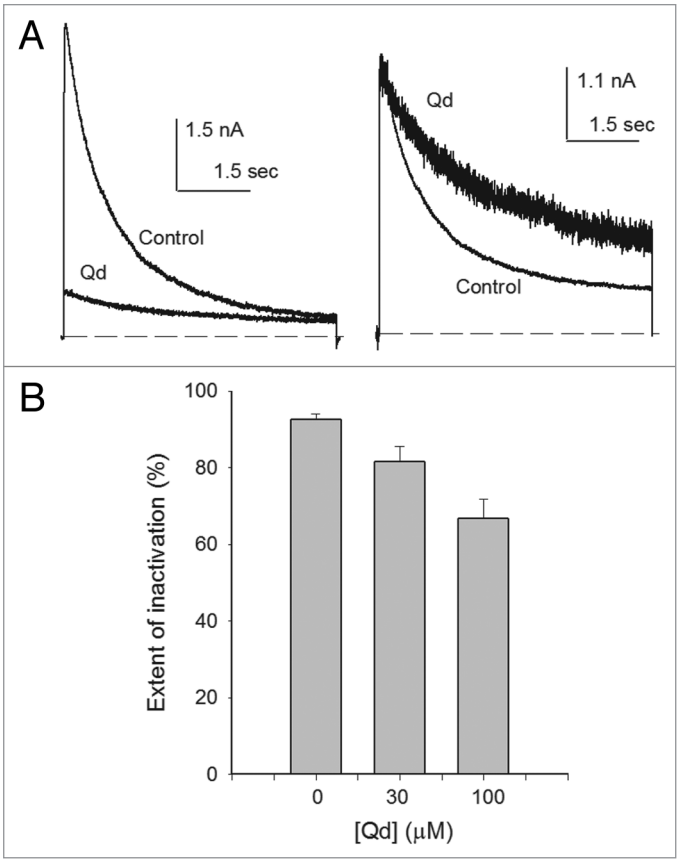


**Figure 5.** Quinidine blockage hinders inactivation. (**A**) Left panel, superimposed Ik evoked by a 0 mV/7 sec pulse either in control 5 $K_o^+$ or in 5 $K_o^+$ + 0.03 mM Qd (trace labeled Qd) solutions. Right panel: $I_K$ with Qd scaled to control peak $I_K$. (**B**) Extent of inactivation vs. [Qd]. The extent of inactivation was evaluated from traces as in (**A**), as: 1-($I_{end}/I_{peak}$), where $I_{peak}$ is peak $I_K$ and $I_{end}$ is $I_K$ at pulse end.

**A kinetic model of Shab inactivation.** The observations reported in this study were synthesized in a kinetic model (**Fig. 6A**). The model is an extension of a kinetic scheme developed to explain the effect of the anti-inflammatory drug celecoxib on Shab channels.[48] The model consists of five closed (Co to C4) and a single open state (O).[49] Inactivation (I) develops from both open and closed states, in a coupled fashion (see *Materials and Methods*). As a result of the different values of inactivation rate constants along the activation pathway (**Table 1**), the probability of inactivation increases as channels approach the open conformation.

Although in the model they are labeled with different numbers, the state I reached from the open and the different closed states should be taken to represent the same inactivated conformation of the protein. Also, as channels do not appreciably conduct during recovery from inactivation, the transition $I_6$ to O was endowed with a small rate (**Table 1**). The model uses data not shown of recovery from inactivation (manuscript in preparation). Note that the model fairly well reproduces channel activation (**Fig. 6B**), as well as inactivation (**Fig. 6C**). Finally, note that the model reproduces both, the apparent U-shaped inactivation curve (**Fig. 6D**), observed with depolarizations that are too short to approach steady-state conditions (0.9 sec), and the Boltzmann $h_\infty$-curve, obtained under near steady-state conditions (20 sec pulses).

## Discussion

Shab channels present a slow inactivation process that develops from the open state with two voltage-independent time constants. In the reference $Na_o$ solution the slower constant has a magnitude (~2 sec) similar to that of Shaker C-type inactivation,[6] and much faster than that of OI of the related Kv2.1 channels,[26,32] under comparable recording conditions.

In addition to OI, Shab also undergoes closed state inactivation. CI develops with a time constant equal to that of the fast OI component (~0.6 sec). Considering that the latter accounts for ~30% of $I_K$ decay during a pulse, and that ~40% of channels do not undergo CI upon delivery of a moderate, 0 mV, pulse from -80 mV, we conclude that although Shab has significant CI it does not have the so called preferential closed state inactivation seen in other Kvs whose inactivation is also facilitated by $K_o^+$.[5,32,50]

This demonstrates that $K_o^+$ facilitation is a property not strictly associated with inactivation processes that preferentially develop from closed states. Additionally, as Shab presents significant CI, our observations also show that the term U-type inactivation is inadequate to denote inactivation process significantly arising from pre-open closed states.

Importantly, we demonstrate that the inactivation curve presents an apparent U-shape when pulse durations are too short to approach steady-state conditions. In contrast, when the inactivating pulse durations are much longer than the slowest inactivation time constant, which allows the channels to approach near steady-state conditions, the inactivation curve ceases to be U-shaped, and it is fitted by the classical $h_\infty$ Boltzmann curve.

The U-shape of the inactivation curves obtained when pulse durations are too short (duration ≤ slowest inactivation time constant) are the result of kinetic processes arising from the relative values of activation and inactivation rates. At more depolarized voltages channel activation is faster, and since inactivation is voltage-independent, and can be reached from both open and closed states (see below), delivering pulses too short to approach steady-state inactivation causes the fewer of these channels to inactivate from closed states during the activating pulse and, because pulse duration is relatively short, they will not have sufficient time to inactivate fully from the open state, yielding the U-shaped curve.

On the other hand, as steady-state conditions are approached channels have enough time to reach a time-invariant extent of inactivation, both from closed and open states, and the U-shape of the curve vanishes. Based on this, and on the extensive discussion of Yue and coworkers,[45] we consider that only in limiting conditions, such as when inactivation arises only from closed states, would a U-shaped curve be observed, near steady-state conditions. On the other hand, when channels inactivate from the open state, but with a very slow rate, approaching near steady-state conditions may be technically difficult to achieve, but this

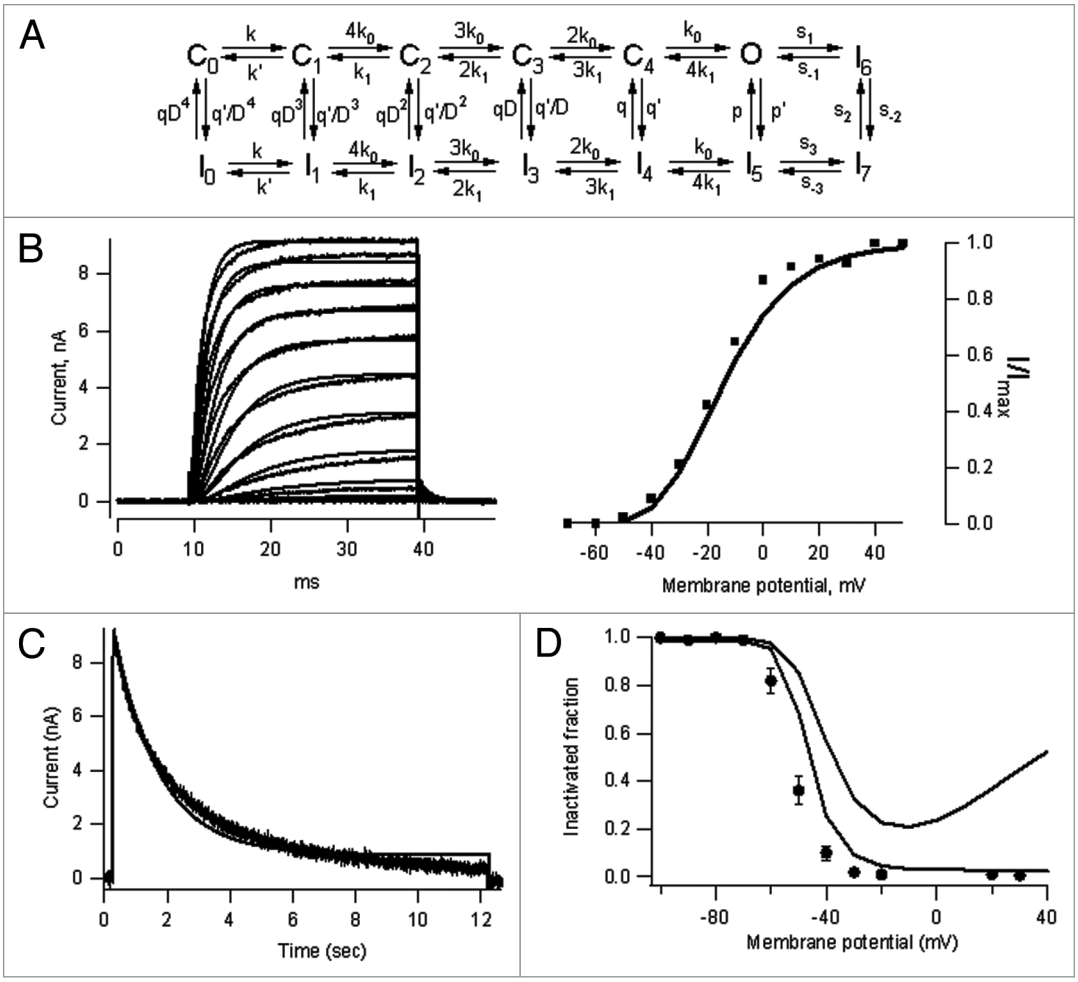


**Figure 6.** A kinetic model of Shab inactivation. (**A**) Kinetic model of Shab inactivation, C, I and O have their standard meaning (see *Materials and Methods* and **Table 1**). (**B**) Comparison of the model predictions with the voltage-dependent activation of Shab channels. The left panel shows good agreement between the model and the data for short activating pulses from –50 to +50 mV. The G-V curve, plotted as a fractional activated current in the right panel is also well explained by the model. (**C**) Model prediction of slow inactivation. For long activating pulses, the model also provides a reasonable good fit of inactivation time course, although it predicts a somewhat larger remaining current at pulse end (Vm = 0 mV). (**D**) Inactivation curve. For long inactivating pulses (12 sec, black trace) the model predicts a monotonically increasing inactivation at depolarized potentials, as contained in the Boltzmann curve, while for shorter pulses (5 sec) a U-shaped inactivation is expected as a consequence of the channel not having reached steady-state during the pulse.

by itself should not vindicate the identification of a particular inactivation as U-type.

Shab inactivation is faster in the presence of either external $K^+$ or TEA. Additionally, we found that when both ions are present, their individual effects are not additive, despite the fact that $TEA_o$ blocks $I_K$ in 100 mM $K^+_o$ as effectively as in $Na_o$. A possible explanation of these observations is that the individual effect of the ions may have reached saturation at the concentrations tested, and that $TEA_o$ and $K_o^+$ speed inactivation by binding to different sites. $TEA_o$ on its blocking site in the external vestibule of the pore,[14] and $K^+$ within the selectivity filter.[51] This proposal is in agreement with the observation that $K_o^+$, but not $TEA_o$, increases the OI rate of Kv2.1 channels.[26,32]

As mentioned before, $TEA_o$ significantly speeds both OI and CI of Shab, and in contrast it does not affect at all the inactivation of the Shab mammalian ortholog Kv2.1.[26] A possible explanation for this difference is that Shab presents a cysteine at the Shaker position 449, a key determinant of the external TEA binding site of Kv channels,[9,14,15] while Kv2.1 presents a tyrosine (Y), at the equivalent position. Tyrosine residues yield a high affinity $TEA_o$ blocking-site,[14] where, interestingly, $TEA_o$ binds without affecting inactivation.[9] This is thought to occur because the Y-binding site seems to hold TEA in a relatively external position, outside the voltage drop across the membrane, as inferred from the voltage-independent $TEA_o$ blockage of pore.[9] In other words, it seems that $TEA_o$ needs to bind deep enough to sense the voltage drop across the membrane, as it does in Shab (data not shown), to either down or upregulate inactivation, as it does in for example Shaker[6] and Shab, respectively.

External $K^+$ significantly speeds Shab OI while in Kv2.1 the same effect is observed although it is less pronounced.[26,32] This

**Table 1.** Kinetic model rate constants

| Rate constants in $s^{-1}$ @ 0 mV | Charge (in $e_o$) |
|---|---|
| ko = 700 | 0.7 |
| k1 = 50 | –0.9 |
| q = 2.2 | 0.7 |
| | |
| q′ = 0.1 | –0.6 |
| p = 0.05 | 0.1 |
| p′ = 0.06 | 0.2 |
| $s_2$ = 35 | 0 |
| $s_{-2}$ = 0.3 | 0 |
| k = 240 | 0.5 |
| | |
| k′ = 130 | –0.5 |
| $s_1$ = 0.03 | 0.1 |
| $s_{-1}$ = 0.1 | –0.1 |
| $s_3$ = 3 | 0 |
| $s_{-3}$ = 7 | 0 |

**Model rate constants.** (A) The voltage-dependence of rate constants is implemented in the model as exponential equations of the form: $k_i(V)=k_i(0)\exp(z_iV / kT)$, where $k_i(V)$ is the rate constant at voltage V, $k_i(0)$ is its value at 0 mV, $z_i$ is the charge associated with the transition and $k$ and T are Boltzmann's constant and the temperature in °K. (B) The value of the allosteric factor D is taken to be 0.3.

similarity suggests that the $K^+$ affinity of the relevant $K^+$ binding site(s) may only be slightly different in both channels, as expected from their conserved signature sequence, and the presence in both channels of the same aminoacid (cysteine) at the Shaker position 463 on S6, a position known to influence $K^+$ binding to the selectivity filter[24] (see below).

As it does on OI, $K_o^+$ also facilitates Shab CI, but in contrast it inhibits the dominant closed state inactivation of Kv2.1.[26] Whatever the cause of this difference may be, it suggests that the relative weights of CI/OI of these channels may not simply be due to their different relative values of inactivation and activation rate constants, but to a qualitative difference on its corresponding CI; even though further work is needed to clarify this point, the differential effects of $K^+$ and TEA on OI/CI of Kv2.1 suggest that inactivation of the latter may be a more complex process than that operating on Shab, as it is also suggested by the regulation of Kv2.1 inactivation by modulatory subunits.[26]

**Role of the central cavity on Shab inactivation.** Quinidine is a lipophilic cation that blocks Shab $I_K$,[47] upon binding to the central cavity of the pore.[47,52-54] Here we show that Qd block hinders Shab inactivation.

Although Qd competes with pore $K^+$ ions, mutually destabilizing their binding,[47] and this effect by itself should be expected to slow down inactivation, the observation that Qd inhibits OI in the presence of only 5 mM $K_o^+$, a [$K^+$] rather low to significantly speed inactivation, suggest that Qd inhibition of inactivation is not the result of a reduced $K^+$ occupancy of the pore. Thus, it appears that Qd binding to the central cavity somehow hinders the Shab inactivation conformational change.

An opposite effect of Qd is observed in C-type inactivating Kv1.4 channels, in which Qd speeds inactivation through an allosteric effect.[55,56] Although further work is needed to fully characterize Qd role on Shab inactivation, its effect appears to be similar to the inhibitory effect of internal TEA on Shaker inactivation and on Kv2.1 OI,[26,27] and hence suggests that involvement of the central cavity may be a common theme in different slow inactivation mechanisms.

**Comparison with C-type inactivation.** Shab inactivation (OI/CI) is accelerated by $K_o^+$ and $TEA_o$. This feature stands in contrast to the characteristic inhibitory effect that these ions exert on C-inactivation,[6-9] which is thought to arise from a steric impediment of a local narrowing of the extracellular entry of the pore that accompanies inactivation,[9,10,12] referred to as the closing of the C-inactivation gate.[5,10,16] In the case of Shab, as well as those Kvs whose inactivation is facilitated by $TEA_o$ and $K_o^+$, the up-modulation effect of these ions is not easily reconciled with a mechanism presenting the C-inactivation narrowing of the extracellular entry of the pore, nor a general significant constriction of the selectivity filter.

Another characteristic of C-inactivation is its dependency on the residues present at the Shaker positions 449 and 463. As mentioned before, Shab presents a cysteine while Shaker has a threonine at position 499. It is known that the mutation T449C on Shaker preserves the hallmarks of C-inactivation.[11] Therefore, it seems unlikely that the differential effects of $TEA_o$ and $K^+_o$ on inactivation of these channels are due to these different residues, at that position on the external vestibule of the pore.

Shaker B presents an alanine at position 463 on S6. It has been reported that the mutation A463C reduces the $K^+$ affinity of the most internal $K^+$ site (s4) of the selectivity filter, and that, as a consequence, $K^+$ occupancy of the externally located site that regulates C-inactivation increases, rendering Shaker inactivation rather insensitive to [$K_o^+$] changes.[24] Shab presents a cysteine at the Shaker 463 equivalent position and its inactivation is appreciably modulated by $K_o^+$ although, as we have shown, in an opposite direction to that in Shaker. This suggests that the $K^+$ site(s) that up-modulate Shab inactivation might not be saturated at low $K_o^+$, as is the case in Shaker A463C. The latter would mean that the presence of a cysteine in Shab does not affect $K^+$ affinity of the pore in the way that it does in Shaker. Alternatively, it might be that $K_o^+$ speeds Shab inactivation in a site(s) different from that at which it inhibits Shaker C-inactivation.

**Shab inactivation: A novel hypothesis regarding slow inactivation mechanisms.** In this study we have shown that $K_o^+$ and $TEA_o$ speed Shab inactivation. On the other hand, we have previously demonstrated that upon exposure to 0 $K^+$ solutions across the membrane the Shab $K^+$ conductance irreversibly collapses with a kinetics that is basically indistinguishable when the channels are either deactivated (Vm = -80 mV) or inactivated (Vm = 0 mV) before their exposure to 0 $K^+$ solutions.[44] It is important to emphasize that in these experiments channels are either deactivated or inactivated in control $K_o^+$-containing solutions, before its subsequent exposure to 0 $K^+$, and that throughout the latter the channels are kept undisturbed at either -80 (deactivated) or

0 mV (inactivated). In other words, this indicates that inactivation does not impede the leak of the stabilizing $K^+$ ion(s) from the Shab pore toward the external solution.[44]

Taken together, the above observations cannot be reconciled, in an obvious manner, with an inactivation mechanism involving a significant narrowing or closing of the extracellular portion of the pore, as it is considered to occur in C-inactivation. Hence, we propose that when Shab inactivates there is only a rearrangement or conformational change of the intracellular side of the pore, affecting the central cavity, which somehow halts $K^+$ conduction. The latter suggests that $K_o^+$ and $TEA_o$ may speed inactivation by allosterically favoring the internally located conformational change of the pore. Moreover, we hypothesize that a similar mechanism may operate in other channels whose slow inactivation is facilitated by external $K^+$, such as Kv2.1 and Kv1.3.

## Materials and Methods

**Cell culture and channel expression.** Sf9 cells grown at 27°C in Grace's media (Gibco) were infected, at a multiplicity of infection of ~10, with a recombinant baculovirus containing Shab $K^+$-channel cDNA (dShab 11), as reported.[57] Experiments were conducted 48 h after the infection.

**Electrophysiological recordings.** Currents were recorded under whole-cell patch-clamp with an Axopatch 1D amplifier (Axon Instruments). The currents were filtered online and sampled at frequencies set to fulfill the Nyquist criteria, with a Digidata 1322A interface. The near steady-state inactivation curve of **Figure 2** was obtained using the gear-shift sampling facility of pClamp 7 using a Digidata 1200 interface (Axon Instruments). Electrodes were made of borosilicate glass (KIMAX 51) pulled to a 1–1.5 MΩ resistance, 80% of the series resistance was compensated. The holding potential (HP) was –80 mV.

**Solutions.** Solutions will be named by their main, test, cation and location across the membrane. The internal $K_i$ solution contained (mM): 30 KCl, 90 KF, 2 $MgCl_2$, 10 EGTA-K, 10 Hepes-K. The $Na_i$ solution contained (mM): 30 NaCl, 90 NaF, 2 $MgCl_2$, 10 EGTA-Na, 10 Hepes-Na. External solutions contained (mM): $Na_o$ (0 $K_o^+$): 145 NaCl, 10 $CaCl_2$, 10 Hepes-Na. $XK_o$: X KCl, 145-X NaCl, 10 $CaCl_2$, 10 Hepes-Na. Fifteen $TEA_o$: 15 TEA-Cl, 130 NaCl, 10 $CaCl_2$, 10 Hepes-Na. The pH of all solutions was 7.2. Quinidine was added to the external 5 $K_o$ solution at the indicated concentrations.

**Data analysis.** The model depicted in **Figure 6** was solved using Runge-Kutta integration implemented in programs written in-house in Igor Pro (Wavemetrics). The time and voltage-dependent occupancy of the open state ($p_o$) was transformed to current according to:

$$I(t,V) = p_0(t,V) \times N \times (V - V_{rev}) \times g_s$$

Where V is the applied voltage, $V_{rev}$ is the reversal potential estimated from the Nernst equation for potassium, $N$ is the number of channels and $g_s$ is the single channel conductance, which we set to be 20 pS.[57]

Points are mean ± SEM of the indicated number of independent experiments. Curves were compared with the extra-sum-of-squares F-test using GraphPad Prism version 5.00 (GraphPad Software, www.graphpad.com). Significance level was set to 0.05.

### Disclosure of Potential Conflicts of Interest

No potential conflicts of interest were disclosed.


### Acknowledgments

This study was performed in partial fulfillment of the requirements of the Doctorate degree in Biomedical Sciences of E.C. at the UNAM. The authors thank J.M. Hernandez for cell culture. This work was supported by DGAPA_UNAM grant IN229712 and CONACYT grant 153504.


### References


1. Aldrich RW. Inactivation of voltage-gated delayed potassium current in molluscan neurons. A kinetic model. Biophys J 1981; 36:519-32; PMID:6275919; http://dx.doi.org/10.1016/S0006-3495(81)84750-9
2. Bean BP. The action potential in mammalian central neurons. Nat Rev Neurosci 2007; 8:451-65; PMID:17514198; http://dx.doi.org/10.1038/nrn2148
3. Hoshi T, Zagotta WN, Aldrich RW. Two types of inactivation in Shaker K+ channels: effects of alterations in the carboxy-terminal region. Neuron 1991; 7:547-56; PMID:1931050; http://dx.doi.org/10.1016/0896-6273(91)90367-9
4. Baukrowitz T, Yellen G. Modulation of $K^+$ current by frequency and external [$K^+$]: a tale of two inactivation mechanisms. Neuron 1995; 15:951-60; PMID:7576643; http://dx.doi.org/10.1016/0896-6273(95)90185-X
5. Kurata HT, Fedida D. A structural interpretation of voltage-gated potassium channel inactivation. Prog Biophys Mol Biol 2006; 92:185-208; PMID:16316679; http://dx.doi.org/10.1016/j.pbiomolbio.2005.10.001
6. López-Barneo J, Hoshi T, Heinemann SH, Aldrich RW. Effects of external cations and mutations in the pore region on C-type inactivation of Shaker potassium channels. Receptors Channels 1993; 1:61-71; PMID:8081712
7. Grissmer S, Cahalan M. TEA prevents inactivation while blocking open K+ channels in human T lymphocytes. Biophys J 1989; 55:203-6; PMID:2784693; http://dx.doi.org/10.1016/S0006-3495(89)82793-6
8. Choi KL, Aldrich RW, Yellen G. Tetraethylammonium blockade distinguishes two inactivation mechanisms in voltage-activated K+ channels. Proc Natl Acad Sci U S A 1991; 88:5092-5; PMID:2052588; http://dx.doi.org/10.1073/pnas.88.12.5092
9. Molina A, Castellano AG, López-Barneo J. Pore mutations in Shaker K+ channels distinguish between the sites of tetraethylammonium blockade and C-type inactivation. J Physiol 1997; 499:361-7; PMID:9080366
10. Yellen G. The moving parts of voltage-gated ion channels. Q Rev Biophys 1998; 31:239-95; PMID:10384687; http://dx.doi.org/10.1017/S0033583598003448
11. Yellen G, Sodickson D, Chen TY, Jurman ME. An engineered cysteine in the external mouth of a K+ channel allows inactivation to be modulated by metal binding. Biophys J 1994; 66:1068-75; PMID:8038379; http://dx.doi.org/10.1016/S0006-3495(94)80888-4
12. Liu Y, Jurman ME, Yellen G. Dynamic rearrangement of the outer mouth of a K+ channel during gating. Neuron 1996; 16:859-67; PMID:8608004; http://dx.doi.org/10.1016/S0896-6273(00)80106-3
13. De Biasi M, Hartmann HA, Drewe JA, Taglialatela M, Brown AM, Kirsch GE. Inactivation determined by a single site in K+ pores. Pflugers Arch 1993; 422:354-63; PMID:8437886; http://dx.doi.org/10.1007/BF00374291
14. Heginbotham L, MacKinnon R. The aromatic binding site for tetraethylammonium ion on potassium channels. Neuron 1992; 8:483-91; PMID:1550673; http://dx.doi.org/10.1016/0896-6273(92)90276-J
15. Luzhkov VB, Aqvist J. Mechanisms of tetraethylammonium ion block in the KcsA potassium channel. FEBS Lett 2001; 495(3):191-6
16. Rasmusson RL, Morales MJ, Wang S, Liu S, Campbell DL, Brahmajothi MV, et al. Inactivation of voltage-gated cardiac K+ channels. Circ Res 1998; 82:739-50; PMID:9562433; http://dx.doi.org/10.1161/01.RES.82.7.739
17. Starkus JG, Kuschel L, Rayner MD, Heinemann SH. Ion conduction through C-type inactivated Shaker channels. J Gen Physiol 1997; 110:539-50; PMID:9348326; http://dx.doi.org/10.1085/jgp.110.5.539
18. Kiss L, LoTurco J, Korn SJ. Contribution of the selectivity filter to inactivation in potassium channels. Biophys J 1999; 76:253-63; PMID:9876139; http://dx.doi.org/10.1016/S0006-3495(99)77194-8
19. Wang Z, Hesketh JC, Fedida D. A high-Na+ conduction state during recovery from inactivation in the potassium channel Kv1.5. Biophys J 2000; 89:23-45

20. Cordero-Morales JF, Cuello LG, Zhao Y, Jogini V, Cortes DM, Roux B, et al. Molecular determinants of gating at the potassium-channel selectivity filter. Nat Struct Mol Biol 2006; 13:311-8; PMID:16532009; http://dx.doi.org/10.1038/nsmb1069
21. Cordero-Morales JF, Jogini V, Lewis A, Vásquez V, Cortes DM, Roux B, et al. Molecular driving forces determining potassium channel slow inactivation. Nat Struct Mol Biol 2007; 14:1062-9; PMID:17922012; http://dx.doi.org/10.1038/nsmb1309
22. Castle NA, Fadous SR, Logothetis DE, Wang GK. 4-Aminopyridine binding and slow inactivation are mutually exclusive in rat Kv1.1 and Shaker potassium channels. Mol Pharmacol 1994; 46:1175-81; PMID:7808439
23. Fedida D, Bouchard R, Chen FS. Slow gating charge immobilization in the human potassium channel Kv1.5 and its prevention by 4-aminopyridine. J Physiol 1996; 494:377-87; PMID:8841998
24. Ogielska EM, Aldrich RW. Functional consequences of a decreased potassium affinity in a potassium channel pore. Ion interactions and C-type inactivation. J Gen Physiol 1999; 113:347-58; PMID:9925829; http://dx.doi.org/10.1085/jgp.113.2.347
25. Jiang XJ, Bett GCL, Li XY, Bondarenko VE, Rasmusson RL. C-type inactivation involves a significant decrease in the intracellular aqueous pore volume of Kv1.4 K+ channels expressed in Xenopus oocytes. J Physiol 2003; 549:683-95; PMID:12730347; http://dx.doi.org/10.1113/jphysiol.2002.034660
26. Kerschensteiner D, Monje F, Stocker M. Structural determinants of the regulation of the voltage-gated potassium channel Kv2.1 by the modulatory α-subunit Kv9.3. J Biol Chem 2003; 278:18154-61; PMID:12642579; http://dx.doi.org/10.1074/jbc.M213117200
27. González-Pérez V, Neely A, Tapia C, González-Gutiérrez G, Contreras G, Orio P, et al. Slow inactivation in Shaker K channels is delayed by intracellular tetraethylammonium. J Gen Physiol 2008; 132:633-50; PMID:19029372; http://dx.doi.org/10.1085/jgp.200810057
28. Olcese R, Latorre R, Toro L, Bezanilla F, Stefani E. Correlation between charge movement and ionic current during slow inactivation in Shaker K+ channels. J Gen Physiol 1997; 110:579-89; PMID:9348329; http://dx.doi.org/10.1085/jgp.110.5.579
29. Loots E, Isacoff EY. Molecular coupling of S4 to a K(+) channel's slow inactivation gate. J Gen Physiol 2000; 116:623-36; PMID:11055991; http://dx.doi.org/10.1085/jgp.116.5.623
30. De Biasi M, Hartmann HA, Drewe JA, Taglialatela M, Brown AM, Kirsch GE. Inactivation determined by a single site in $K^+$ pores. Pflugers Arch 1993; 422:354-63; PMID:8437886; http://dx.doi.org/10.1007/BF00374291
31. Villalba-Galea CA, Sandtner W, Starace DM, Bezanilla F. S4-based voltage sensors have three major conformations. Proc Natl Acad Sci U S A 2008; 105:17600-7; PMID:18818307; http://dx.doi.org/10.1073/pnas.0807387105
32. Klemic KG, Shieh CC, Kirsch GE, Jones SW. Inactivation of Kv2.1 potassium channels. Biophys J 1998; 74:1779-89; PMID:9545040; http://dx.doi.org/10.1016/S0006-3495(98)77888-9
33. Cheng YM, Azer J, Niven CM, Mafi P, Allard CR, Qi J, et al. Molecular determinants of U-type inactivation in Kv2.1 channels. Biophys J 2011; 101:651-61; PMID:21806933; http://dx.doi.org/10.1016/j.bpj.2011.06.025
34. Klemic KG, Kirsch GE, Jones SW. U-type inactivation of Kv3.1 and Shaker potassium channels. Biophys J 2001; 81:814-26; PMID:11463627; http://dx.doi.org/10.1016/S0006-3495(01)75743-8
35. Butler A, Wei AG, Baker K, Salkoff L. A family of putative potassium channel genes in *Drosophila*. Science 1989; 243:943-7; PMID:2493160; http://dx.doi.org/10.1126/science.2493160
36. Wei A, Covarrubias M, Butler A, Baker K, Pak M, Salkoff LK. K+ current diversity is produced by an extended gene family conserved in *Drosophila* and mouse. Science 1990; 248:599-603; PMID:2333511; http://dx.doi.org/10.1126/science.2333511
37. Singh S, Wu CF. Properties of potassium currents and their role in membrane excitability in *Drosophila* larval muscle fibers. J Exp Biol 1990; 152:59-76; PMID:2121887
38. Quattrocki EA, Marshall J, Kaczmarek LK. A Shab potassium channel contributes to action potential broadening in peptidergic neurons. Neuron 1994; 12:73-86; PMID:8292361; http://dx.doi.org/10.1016/0896-6273(94)90153-8
39. Tsunoda S, Salkoff L. Genetic analysis of *Drosophila* neurons: Shal, Shaw, and Shab encode most embryonic potassium currents. J Neurosci 1995a; 15:1741-54; PMID:7891132
40. Tsunoda S, Salkoff L. The major delayed rectifier in both *Drosophila* neurons and muscle is encoded by Shab. J Neurosci 1995b; 15:5209-21; PMID:7623146
41. Ueda A, Wu CF. Distinct frequency-dependent regulation of nerve terminal excitability and synaptic transmission by $I_A$ and $I_K$ potassium channels revealed by *Drosophila* Shaker and Shab mutations. J Neurosci 2006; 26:6238-48; PMID:16763031; http://dx.doi.org/10.1523/JNEUROSCI.0862-06.2006
42. Peng IF, Wu CF. Differential contributions of Shaker and Shab K+ currents to neuronal firing patterns in *Drosophila*. J Neurophysiol 2007; 97:780-94; PMID:17079336; http://dx.doi.org/10.1152/jn.01012.2006
43. Frolov RV, Berim IG, Singh S. Inhibition of delayed rectifier potassium channels and induction of arrhythmia: a novel effect of celecoxib and the mechanism underlying it. J Biol Chem 2008; 283:1518-24; PMID:17984087; http://dx.doi.org/10.1074/jbc.M708100200
44. Gómez-Lagunas F. Stability of the Shab K+ channel conductance in 0 K+ solutions: the role of the membrane potential. Biophys J 2007; 93:4197-208; PMID:17704149; http://dx.doi.org/10.1529/biophysj.106.095794
45. Patil PG, Brody DL, Yue DT. Preferential closed-state inactivation of neuronal calcium channels. Neuron 1998; 20:1027-38; PMID:9620706; http://dx.doi.org/10.1016/S0896-6273(00)80483-3
46. Chen J, Avdonin V, Ciorba MA, Heinemann SH, Hoshi T. Acceleration of P/C-type inactivation in voltage-gated K(+) channels by methionine oxidation. Biophys J 2000; 78:174-87; PMID:10620284; http://dx.doi.org/10.1016/S0006-3495(00)76583-0
47. Gomez-Lagunas F. Quinidine interaction with Shab K+ channels: pore block and irreversible collapse of the K+ conductance. J Physiol 2010; 588:2691-706; PMID:20547671; http://dx.doi.org/10.1113/jphysiol.2010.193128
48. Arias-Olguin II, Carrillo E, Meza-Torres B, Barriga-Montoya C, Balleza D, Gomez-Lagunas F. Induction of a fast inactivation gating on delayed rectifier Shab K(+) channels by the anti-inflammatory drug celecoxib. Channels (Austin) 2011; 5:56-64; PMID:21084865; http://dx.doi.org/10.4161/chan.5.1.13972
49. Zagotta WN, Hoshi T, Aldrich RW. Shaker potassium channel gating. III: Evaluation of kinetic models for activation. J Gen Physiol 1994; 103:321-62; PMID:8189208; http://dx.doi.org/10.1085/jgp.103.2.321
50. Bähring R, Covarrubias M. Mechanisms of closed-state inactivation in voltage-gated ion channels. J Physiol 2011; 589:461-79; PMID:21098008; http://dx.doi.org/10.1113/jphysiol.2010.191965
51. Doyle DA, Morais Cabral J, Pfuetzner RA, Kuo A, Gulbis JM, Cohen SL, et al. The structure of the potassium channel: molecular basis of K+ conduction and selectivity. Science 1998; 280:69-77; PMID:9525859; http://dx.doi.org/10.1126/science.280.5360.69
52. Yeola SW, Rich TC, Uebele VN, Tamkun MM, Snyders DJ. Molecular analysis of a binding site for quinidine in a human cardiac delayed rectifier K+ channel. Role of S6 in antiarrhythmic drug binding. Circ Res 1996; 78:1105-14; PMID:8635242; http://dx.doi.org/10.1161/01.RES.78.6.1105
53. Zhang H, Zhu B, Yao JA, Tseng GN. Differential effects of S6 mutations on binding of quinidine and 4-aminopyridine to rat isoform of Kv1.4: common site but different factors in determining blockers' binding affinity. J Pharmacol Exp Ther 1998; 287:332-43; PMID:9765354
54. Caballero R, Pourrier M, Schram G, Delpón E, Tamargo J, Nattel S. Effects of flecainide and quinidine on Kv4.2 currents: voltage dependence and role of S6 valines. Br J Pharmacol 2003; 138:1475-84; PMID:12721103; http://dx.doi.org/10.1038/sj.bjp.0705199
55. Wang S, Morales MJ, Qu YJ, Bett GC, Strauss HC, Rasmusson RL. Kv1.4 channel block by quinidine: evidence for a drug-induced allosteric effect. J Physiol 2003; 546:387-401; PMID:12527726; http://dx.doi.org/10.1113/jphysiol.2002.029512
56. Bett GC, Rasmusson RL. Inactivation and recovery in Kv1.4 K+ channels: lipophilic interactions at the intracellular mouth of the pore. J Physiol 2004; 556:109-20; PMID:14608006; http://dx.doi.org/10.1113/jphysiol.2003.055012
57. Islas LD, Sigworth FJ. Voltage sensitivity and gating charge in Shaker and Shab family potassium channels. J Gen Physiol 1999; 114:723-42; PMID:10539976; http://dx.doi.org/10.1085/jgp.114.5.723